A New Muscle Contractile System Composed of a Thick Filament Lattice and a Single Actin Filament

Madoka Suzuki,* Hideaki Fujita,† and Shin'ichi Ishiwata*‡§

*Department of Physics, School of Science and Engineering, Waseda University, Tokyo, Japan; †Tohoku University Biomedical Engineering Research Organization, Miyagi, Japan; and ‡Advanced Research Institute for Science and Engineering, and §Consolidated Research Institute for Advanced Science and Medical Care, Waseda University, Tokyo, Japan

ABSTRACT To bridge the gap between the contractile system in muscle and in vitro motility assay, we have devised an A-band motility assay system. A glycerinated skeletal myofibril was treated with gelsolin to selectively remove the thin filaments and expose a single A-band. A single bead-tailed actin filament trapped by optical tweezers was made to interact with the inside or the outer surface of the A-band, and the displacement of the bead-tailed filament was measured in a physiological ionic condition by phase-contrast and fluorescence microscopy. We observed large back-and-forth displacement of the filament accompanied by a large change in developed force. Despite this large tension fluctuation, we found that the average force was proportional to the overlap inside and outside the A-band up to ~150 nm and 300 nm from the end of the A-band, respectively. Consistent with the difference in the density of myosin molecules, the average force per unit length of the overlap inside the A-band (the time-averaged force/myosin head was ~1 pN) was approximately twice as large as that outside. Thus, we conclude that the A-band motility assay system described here is suitable for studying force generation on a single actin filament, and its sliding movement within a regular three-dimensional thick filament lattice.

INTRODUCTION

Mechanically (1,2) or chemically (3–5) skinned muscle fibers and myofibrils (6,7) have long been used in muscle physiology to study properties of the interaction between actin and myosin. Such muscle models have provided important information about the molecular mechanisms in both skeletal and cardiac muscle contraction. However, since the development of the in vitro motility assay (8,9) and single-molecule imaging (10,11) and manipulation (12,13) techniques, these new systems and techniques have been widely used to study sliding movement and force generation on a single actin filament and myosin molecules (14). Such studies are indispensable for direct measurements of force, working stroke, and the kinetics of each single molecular interaction (15–22). Although the sliding mechanism of muscle contraction appeared established from reports after the introduction of in vitro systems, some differences have since been found between muscle models and in vitro systems. For example, there are interesting phenomena observed only in muscle model systems, such as stretch activation and spontaneous oscillatory contraction (23). These phenomena are probably attributable to the characteristics of a high-ordered system. Myosin molecules in in vitro systems are usually adhered to glass or bead surfaces two-dimensionally in a random fashion, and there seem to be some myosin molecules with only one head available (17). Therefore, as an actin filament tends to detach from myosin heads, especially at physiological conditions characterized by higher ionic strength, experimental conditions must be limited to low ionic strength. These limitations could be critical for studying the mechanism of muscle contraction that occurs in an ordered array of myofilaments. In fact, it is reported that force generation largely depends on the orientation of myosin molecules (24) and ionic conditions.

Here, we present a new motility assay system in which a single actin filament is pulled into a thick-filament lattice. This system, which we call an A-band motility assay system or ''bionanomuscle'', is composed of a single actin filament and the A-band, where the lattice structure of myosin thick filaments is maintained. We hope to answer some long-standing questions in muscle physiology, such as whether the myosin molecule is an independent force generator irrespective of the conditions, or if there is cooperativity in force generation and its regulatory mechanisms.

In this study, we have succeeded in measuring the force and determining a length-force relationship for a single actin filament working in an organized structure, i.e., a thick-filament lattice. We observed large fluctuations in force development and the displacement of an actin filament around the mean values. This phenomenon is related to what Borejdo and Morales (25) intended to record to characterize individual cross-bridge functions in muscle fibers. Some results we obtained at the preliminary stage of this project, and which are not included here, have been published (26).

MATERIALS AND METHODS

Preparation of myofibrils and proteins

All procedures were performed according to the Regulations for Animal Experimentation at Waseda University. Male white rabbits (2.0–2.5 kg)

Submitted October 22, 2004, and accepted for publication January 14, 2005.

Address reprint requests to Shin'ichi Ishiwata, Dept. of Physics, School of Science and Engineering, Waseda University, 3-4-1 Okubo, Shinjuku-ku, Tokyo 169-8555, Japan. Tel.: 81-3-5286-3437; Fax.: 81-3-5286-3437; E-mail: ishiwata@waseda.jp.

0006-3495/05/07/321/08 $2.00

doi: 10.1529/biophysj.104.054957

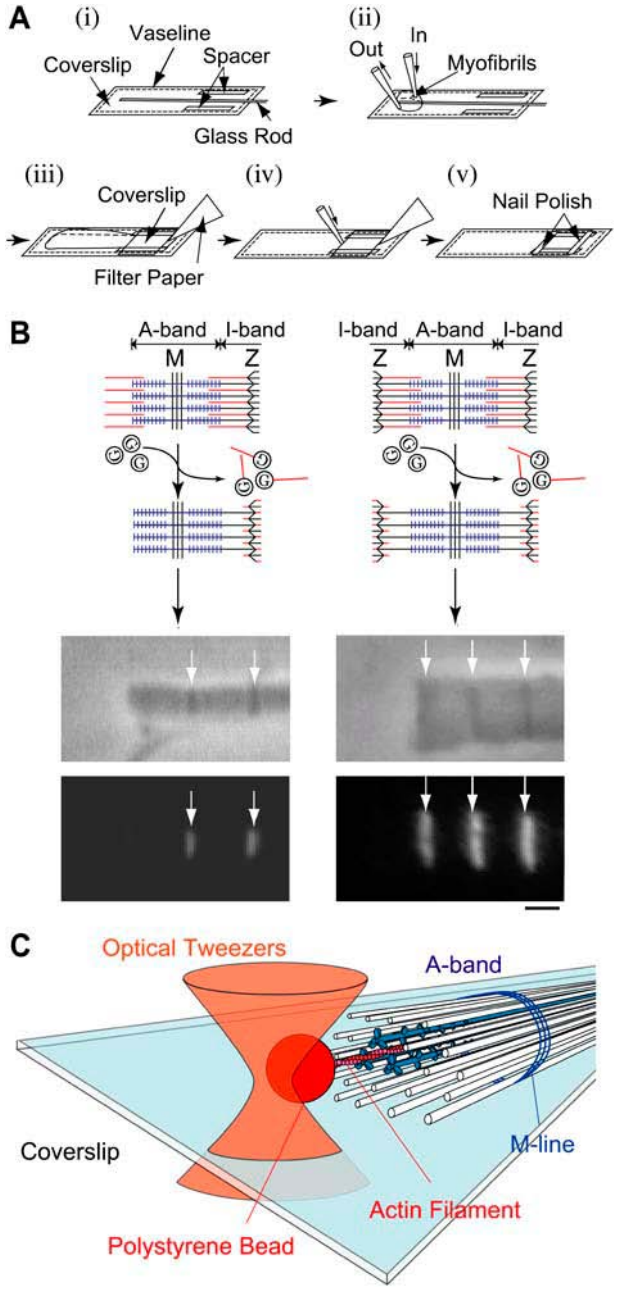

FIGURE 1 (*A*) Procedure for preparing the A-band motility assay system on a coverslip. A thin glass rod prepared by heating and stretching a glass micropipette was employed to exchange the solution smoothly without sucking up myofibrils (see text). (*B*) Schematic diagram illustrating the longitudinal section of the A-band motility assay system (*upper*) and snap shots (*lower*) obtained after the gelsolin treatment of myofibrils, to which a bead-tailed actin filament trapped with optical tweezers was approached from the left. (*Left*) A myofibril used for the experiments. (*Right*) A small bundle of myofibrils not used for the experiments. Myofibrils prepared from glycerinated rabbit psoas muscle fibers were exposed to gelsolin (*Gs in circles*), so that the thin filaments (*red line*) were selectively removed. Snap shots show phase-contrast (*top*) and fluorescence (*bottom*) images of a myofibril (*left*) and a small bundle of myofibrils (*right*) after the gelsolin treatment. Myofibrils were labeled with Rh-Ph after the gelsolin treatment to identify the position of the Z-lines. Every image was obtained by integrating for 1 s (30 frames). Arrows indicate the Z-lines. Scale bar, 1 μm. (*C*) Schematic three-dimensional illustration of the A-band motility assay system. A bead-tailed actin filament was brought into contact with the edge of the exposed A-band using optical tweezers.

were anesthetized with sodium pentobarbital (150 mg/kg). The body, in which psoas, back, and leg muscles were exposed, was incubated in crushed ice for 15 min. Myofibrils were prepared by homogenizing glycerinated rabbit psoas muscle fibers in rigor solution (60 mM KCl, 5 mM $MgCl_2$, 10 mM 3-(*N*-morpholino)propanesulfonic acid (MOPS), pH 7.0, and 1 mM EGTA). Glycerination was performed as described previously (27). G-actin was prepared from rabbit white skeletal muscle (28). Actin filaments were labeled with rhodamine-phalloidin (Rh-Ph, R-415; Molecular Probes, Eugene, OR). The bead-tailed actin filament, i.e., an actin filament with the barbed (B-) end attached to a 1-μmϕ, carboxylate-modified polystyrene bead (08226-15, Polysciences, Warrington, PA) through gelsolin, was prepared as previously reported (17,29). Bovine plasma gelsolin was prepared according to the method of Kurokawa et al. (30); during this preparation, the incubation time of gelsolin in Ca^{2+}-free buffer was shortened as much as possible because severing activity was lowered by incubation in the Ca^{2+}-free buffer. The concentrations of free Mg^{2+}, MgATP, MgADP, and other chemicals were calculated by computer, using the published values for stability constants (31).

Microscopy

The microscopy system and the method for image analysis were basically the same as those reported previously (17), with some modifications as follows: The phase-contrast image of the bead, acquired with a CCD camera (CCD-300, Dage-MTI, Michigan City, IN), was stored in a personal computer (Apple Japan, Tokyo, Japan) with a frame grabber LG3 (National Institutes of Health, Washington, DC). The bead position was determined from digitized camera frames having a 30/s sampling video rate. Fluorescence images of an actin filament and a bead were visualized using an ICCD camera (ICCD-350F, Video Scope International, Washington, DC). An Nd:YAG laser (T10-V-106C, 2.5 W, Spectra-Physics Lasers, Mountain View, CA) was used as the optical tweezers. The stiffness of the optical tweezers, 0.10–0.25 pN/nm, was determined as described previously (32). On the other hand, we estimated the spatial resolution of the data obtained at a time resolution of 1/30 s, because the movement of the bead was recorded at the video rate (see Nishizaka et al. (17)). Thus, the standard deviation of the fluctuation of the position of the bead trapped for 40 s by the optical tweezers with a stiffness of 0.12 pN/nm was 1.43 nm in the x direction and 1.46 nm in the y direction ($n = 9$). The SD of the fluctuation of the position of the bead attached to a glass surface for 40 s was 2.15 nm in the x direction and 1.71 nm in the y direction ($n = 9$).

Preparation of the A-band motility assay system

As schematically illustrated in Fig. 1, our A-band motility assay system was prepared by removing the thin filaments selectively from a single or a small bundle of myofibrils with gelsolin treatment on ice (33–35). First, an embankment was made with Vaseline along the edge of the coverslip to keep the solution from spilling. Spacers 75 μm thick, and a glass rod made by heating and stretching a 100-μl glass micropipette (2-000-100, Drummond Scientific, Broomall, PA) were placed as illustrated in Fig. 1 *A i*. We found that a glass rod was useful for carefully changing the solution without sucking up myofibrils, because it worked as an obstacle, preventing myofibrils from flowing.

Second, the suspension of myofibrils (100 μl) in a rigor solution was placed on one side of a coverslip (Fig. 1 *A ii*) and the rigor solution was slowly exchanged with a gelsolin solution A (60 mM KCl, 4 mM $MgCl_2$, 20 mM MOPS, pH 7.0, 2 mM EGTA, 1.9 mM $CaCl_2$ (pCa ~5), 1.5 mM NaN_3, 2 mM leupeptin, and 0.3 mg/ml gelsolin) using a pair of micropipettes

and taking care not to suck up myofibrils. After 30 min of gelsolin treatment, the gelsolin solution A was exchanged with the gelsolin solution B (gelsolin solution A plus 20 mM 2,3-butanedione 2-monoxime and 1 mM ATP) using a pair of micropipettes. After 20 min of treatment, the myofibrils were washed first with a relaxing solution (120 mM KCl, 4 mM $MgCl_2$, 20 mM MOPS, pH 7.0, 4 mM EGTA, 4 mM ATP, and 10 mM dithiothreitol (DTT)), and then with a rigor solution containing 10 mM DTT. Then, after the glass rod was removed, the whole area surrounded by the embankment of Vaseline was filled with the rigor solution containing DTT (Fig. 1 *A iii*). A flow cell was made by putting a smaller coverslip on spacers placed on the other side of the larger coverslip. The solution was then sucked by a piece of filter paper to move the A-band toward the flow cell, which resulted in the attachment of the A-band to the surface of a larger coverslip, where gelsolin was not present. In this step, it was essential to attach the A-band to the glass surface where gelsolin treatment had not been carried out. The bead-tailed actin filament tended to be cut when the experiments were performed at the place where the gelsolin treatment was done, probably because free gelsolin molecules attached to the glass surface could not be washed away. During this procedure, myofibrils aligned in the same orientation along the flow line. The A-band assay system thus prepared was treated with 0.5% (v/v) Triton X-100 in the rigor solution containing 10 mM DTT and then washed several times with the rigor solution containing 10 mM DTT to remove Triton X-100 (Fig. 1 *A iv*). This wash is important for thoroughly washing away contaminating gelsolin. All procedures were carried out on ice.

Finally, we mounted the flow cell on the stage of a microscope and attempted to find the A-band motility assay system appropriate for the following experiments. The Z-line of the exposed A-band at the end of a myofibril should be absent. If necessary, a fresh rigor solution with DTT was poured into the flow cell during the search as the solution in the flow cell was easily evaporated. After an appropriate A-band was selected, the flow cell was washed with an assay buffer (100 mM KCl, 4.2 mM $MgCl_2$ (free $Mg^{2+} = 2$ mM), 25 mM imidazole-HCl, pH 7.4, 1 mM EGTA, 2.2 mM ATP (MgATP = 2 mM), 0.5 mg/ml bovine serum albumin, 10 mM DTT, 4.5 mg/ml D(+)-glucose, 50 units/ml glucose oxidase, 50 units/ml catalase, 15 mM creatine phosphate and 150 units/ml creatine phosphokinase). Then, the bead-tailed actin filaments in the assay buffer were applied, and both edges of the flow cell were sealed with nonfluorescent nail polish (Fig. 1 *A v*). All the experiments were carried out at 27–29°C.

RESULTS

Development of the A-band motility assay system

The ends of the myofibrils have either exposed A-bands (the left column of Fig. 1 *B*) or Z-lines (the right column of Fig. 1 *B*) as myofibrils tend to be cut at the I-band during homogenization in the rigor solution. As shown in Fig. 1 *B*, the Z-line was observable as a black line in a phase-contrast image and a bright line in a fluorescent image. (Here, short actin filaments remaining at the Z-line were fully labeled with Rh-Ph after the gelsolin treatment. In most observations, the Z-line became weakly fluorescent by the binding of free Rh-Ph molecules in the actin solution (Fig. 2).) We could confirm that exposed A-bands maintained their original thickness (usually >1 μm) by referring to a phase-contrast image of a bead 1 μm in diameter attached to the glass surface. It is to be noted that some preparations were composed of a few myofibrils (see the micrograph in the right column of Fig. 1 *B*), so that these preparations were thicker than 2 μm. The A-band motility assay system we devised is schematically illustrated in Fig. 1 *C*.

In some gelsolin-treated myofibrils, the A-bands were shorter than 1.6 μm, probably because the thick filaments were partially depolymerized from the ends (36). Also, in some preparations both ends of the A-bands looked dense under the phase-contrast microscope. This dense material may be attributable to the folded ends of thick filaments and/or some materials that were not successfully removed by homogenization (33). Some of the A-bands looked faint under the phase-contrast microscope, probably because the thick-filament lattice was partially disorganized (37). These preparations were not used in the experiments.

Even in A-bands that have not looked like those described above, we were concerned that folded connectin/titin molecules might have been present at the end of the thick filaments, because such folded molecules could interrupt the entrance of actin filaments into the thick-filament lattice. However, we concluded from the following observations that there were no obstacles interacting with actin filaments at the edge of the A-band:

1. When a bead-tailed actin filament interacted with the surface of the end-plane, which is perpendicular to the long axis of the A-band, we observed an active force development (data not shown).
2. Actin filaments could slide on the surface (including the surface of the end-plane) of the A-band.
3. Actin filaments were pulled out smoothly from the end of the A-band in addition to their smooth entrance into the A-band.

Force measurement with the A-band motility assay system

A bead-tailed actin filament of ~1–3 μm long was trapped with optical tweezers and brought to the edge of an exposed A-band by moving the sample stage. To examine force generation at the outer surface of the A-band, the trapped bead was brought to the corner of the exposed A-band. The height of the bead from the coverslip was adjusted by comparing the phase-contrast images of the A-band and the bead, so that the actin filament interacted with the outside of the A-band (Fig. 2 *A*).

To examine the force generation inside the A-band, the trap center was set near the end plane of the A-band, such that the actin filament did not reach the A-band. The position of the trap center was carefully selected to be located at the center of the end-plane of the A-band not only laterally but also in depth. Here, we made sure that the bead did not attach to the glass surface. Then, with the use of a stepping motor on the sample stage, the A-band was moved in 25-nm steps toward the bead held in the trap center. Insofar as the actin filament did not interact with the A-band, the trapped bead freely rotated in the trap (a movie is available at http://www.phys.waseda.ac.jp/bio/ishiwata/movies/sfibj2004movie1.avi). If the interaction did not occur even when the actin filament was pointed at the A-band, the sample stage was moved

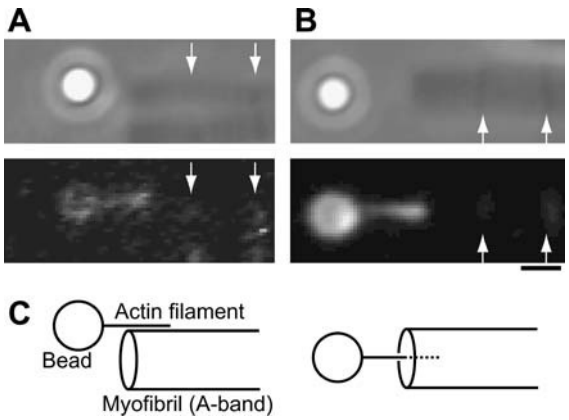

FIGURE 2 Phase-contrast (*top*) and fluorescence (*bottom*) images of the A-band motility assay system. (*A*) An actin filament made to interact with the outer surface of the A-band. (*B*) An actin filament interacting with the end-plane of the A-band (a movie is available at http://www.phys.waseda.ac.jp/bio/ishiwata/movies/sfibj2004movie1.avi). (*C*) Schematic illustrations representing the arrangement of the bead-tailed actin filament and the A-band in *A* and *B*, respectively. Unlike in Fig. 1 *B*, the Z-lines have become observable because of free Rh-Ph with bead-tailed actin filaments. Even when the Z-lines were less labeled, the brightness was enough to identify the Z-lines in fluorescence images (*bottom*). Every image was obtained by integrating for 1 s (30 frames). A part of an actin filament near the bead is photobleached, probably due to two-photon illumination (532 nm) by the laser light used for the optical tweezers. Arrows indicate the Z-lines. Scale bar, 1 μm.

further to bring the A-band closer to the bead. When the pointed end of the actin filament touched the A-band, a force began to be generated, so that the actin filament was pulled into the A-band (Fig. 1 *C*). If necessary, the position of the sample stage was adjusted to make the actin filament parallel to the long axis of the A-band and to the glass surface (Fig. 2 *B*).

As soon as the bead-tailed actin filament touched the outer surface of the A-band (Fig. 3, *A* and *B*) or the end-plane of the A-band (Fig. 3, *C* and *D*), the actin filament began to slide quickly (cf. Fig. 3, *A* and *D*) toward the center of the A-band, i.e., the M-line region. The sliding of the actin filament continued, accompanied by changes in the overlapping length and load (this is a so-called auxotonic condition). At the steady level, the force generated by myosin molecules in the A-band needs to balance the load applied by the optical tweezers. When an actin filament interacted with the outer surface of the A-band, a sudden detachment of the filament from the A-band sometimes occurred, so that the bead was returned to the trap center. Even after the force reached a steady state, fluctuations in the overlapping length and the force continued (usually as much as ± 30 nm and sometimes $\sim \pm 50$ nm for the displacement, and up to ± 10 pN for the force around the average position). It should be noted here that the extent of these fluctuations is much larger than a measurement error (cf. Materials and Methods).

Several seconds after a steady state was attained, either the laser power was suddenly changed (Fig. 4 *A*, method 1) or the sample stage was stepwise moved in parallel to the long axis of the A-band (Fig. 4 *B*, method 2). By repeating this procedure, we could successively obtain new steady levels. Examples of data from the former and latter methods are shown in Fig. 3, *A* and *C*, and *B* and *D*, respectively. These experiments were designed to determine the length-force relationship.

As expected from the mechanical constraints schematically shown in Fig. 4, the larger the stiffness of the optical tweezers, the smaller the amount of the displacement. Also, a steady level does not exist unless the stiffness of the optical tweezers is larger than the slope of the length-force relationship of the A-band. In practice, the bead often escaped from the optical trap and slid into the A-band when the stiffness of the optical tweezers was lowered.

Length-force relationship

Fig. 5, *A* and *C*, show relationships between the displacement of the bead and the change in the generated force due to the change in overlap of an actin filament and the A-band. The point, where the developed and trapping forces were on average balanced was plotted on the ordinate. The average forces then obtained after stepwise changing the stiffness of the optical tweezers (method 1) or moving the sample stage (method 2) were plotted to the right or the left depending on whether the actin filament slid into or was pulled out from the A-band, respectively. Because each set of data obtained in each experiment appeared to be linear, each set was simulated by a straight line. The data obtained by methods 1 and 2 were indistinguishable from each other. The intercept with the abscissa of the straight line indicates the initial length of the overlap of the actin filament with the A-band (cf. Fig. 4). Correspondingly, the intercept with the ordinate of the straight line shows the average force initially developed. From the average slope of the data shown in Fig. 5, *A* and *C*, we obtained the force per unit length of overlap when an actin filament interacts with the outer surface or the end plane, respectively, of the A-band (Table 1). The former was determined as 0.097 ± 0.032 pN/nm (mean $\pm$ SE. of the slopes, $n = 10$), and the latter as 0.16 ± 0.051 pN/nm (mean $\pm$ SE, $n = 13$). We confirmed that these two sets of data were significantly different from each other (significance, $0.01 < P < 0.05$, verified by Kolmogorov-Smirnov test, and $P < 0.01$, verified by Mann-Whitney U-test).

Then, each set of data was moved parallel to the abscissa until the straight line obtained by the least-squares method extrapolated the origin (Fig. 5, *B* and *D*, for *A* and *C*, respectively). These procedures converted the relationship between the change in overlap and the average force (Fig. 5, *A* and *C*) to the overlapping length of actin filament with the A-band versus the average force (Fig. 5, *B* and *D*). Fig. 5 *B*, obtained from Fig. 5 *A*, shows linear relationship, but the data in Fig. 5 *D* were broadly distributed.

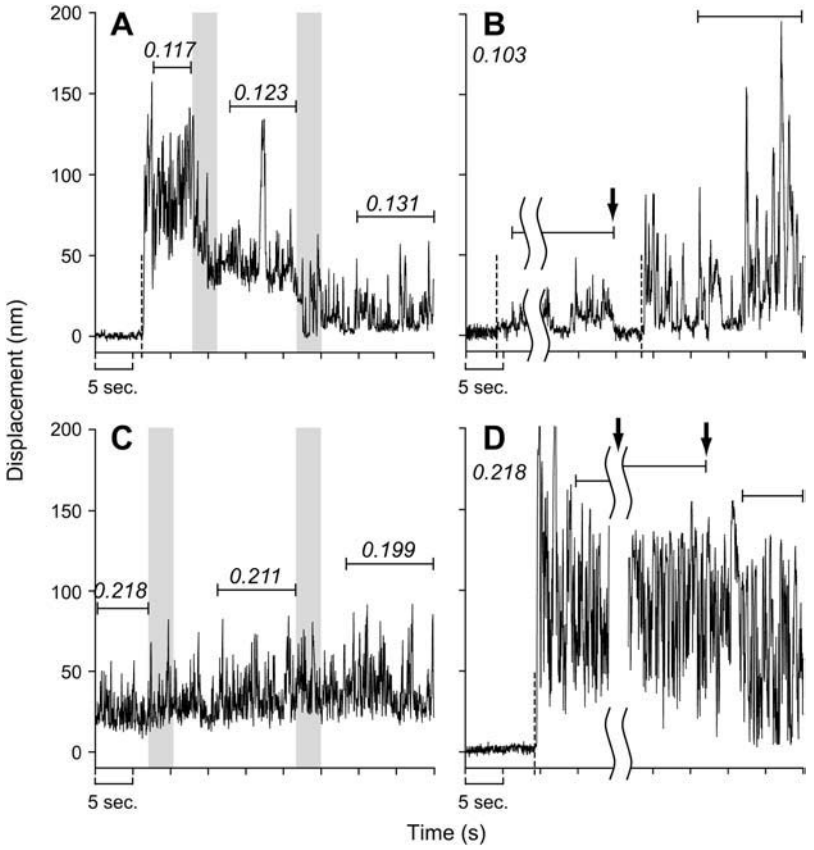

FIGURE 3 Time course of the displacement of a trapped bead in the A-band motility assay system. (*A* and *B*) An actin filament interacting with the outer surface of the A-band, corresponding to the situation shown in Fig. 2 *A*. (*C* and *D*) An actin filament interacted inside the A-band, corresponding to the situation shown in Fig. 2 *B*. At first, the bead stayed at the center of the trap (*A*, *B*, and *D*). The actin filament began to interact with the A-band at the moment shown by the broken lines. While the actin filament was interacting with the A-band, the laser power for the optical tweezers was changed to alter the stiffness of the optical tweezers (*A* and *C*), or the sample stage was moved stepwise (*B* and *D*). The average position of the bead was determined in the region indicated by solid horizontal lines. The italic figures indicate the stiffness of the optical tweezers (pN/nm). The gray rectangles in *A* and *C* show the period during which the laser power was changed. The arrows in *B* and *D* show the moment at which the sample stage was moved stepwise.

DISCUSSION

Average force generated by single myosin heads

In general, 95% of the data are included in the region surrounded by mean ± SE × 1.96. Therefore, 95% of the data of the slope shown in Fig. 5 *A* are included in the region surrounded by the dashed lines of 0.097 ± (0.032 × 1.96) pN/nm (Fig. 5 *B*). On the other hand, the data in Fig. 5 *D* appeared to be classified into two groups having different slopes. Because the smaller slope is nearly equal to that for Fig. 5 *B*, we tested whether a significant difference exists between the group having the smaller slope and the data in Fig. 5 *B*. Statistical analysis demonstrated no significant difference between the data in the region of 0.097 ± (0.032 × 1.96) pN/nm (the region surrounded by the *dashed lines*) in Fig. 5 *D* and those in Fig. 5 *B* ($P \sim 0.25$, verified by Mann-Whitney U-test). Thus, we conclude that the data classified into the group having the smaller slope in Fig. 5 *D* are attributable to the actin filaments interacting outside the A-band (or at an equivalent geometry; most probably the outer surface of the A-band located within a small bundle of myofibrils). Concerning the rest of the data, they were

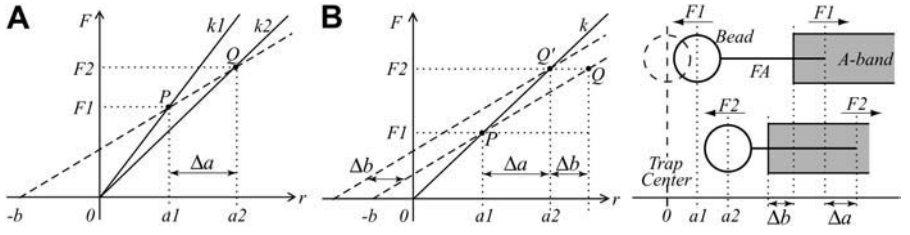

FIGURE 4 Methods to determine the balancing points by changing the stiffness of the optical tweezers (*A*, method 1), or moving the sample stage (*B*, method 2). Abscissa, displacement of the bead from the trap center ($r = 0$); ordinate, trapping force (*solid line*) or the force developed on an actin filament interacting with the A-band (*dashed line*); k, k_1, and k_2, stiffness of the optical tweezers; a_1 and a_2, displacement of the bead from the trap center, and $\Delta a = |a_1 - a_2|$; b, the initial length of the overlap between an actin filament and the A-band; Δb, displacement of the sample stage. (*A*) After the developed force (*dashed line*) and load (*solid line* k_1) are balanced at point P(a_1, F_1), the stiffness of the optical tweezers is changed from k_1 to k_2, which results in a shift of the balancing point from P to Q(a_2, F_2). The slope of the broken line, i.e., the force per unit length of overlap, is determined by $|F_2 - F_1|/\Delta a$. (*B, left*) At first, the developed force on the actin filament (*broken line* crossing the abscissa at $-b$) and the load applied by the optical tweezers (*solid line k*) are balanced at $P(a_1, F_1)$. When the sample stage is shifted toward the trap center by Δb, the balancing point moves to the point $Q'(a_2, F_2)$. Therefore, the slope of the broken line, i.e., the force per unit length of the overlap, passing through the points P and Q($a_2 + \Delta b$, F_2) is determined by $|F_1 - F_2|/(\Delta a + \Delta b)$. (*B*, *right*) Schematic illustration of this procedure.

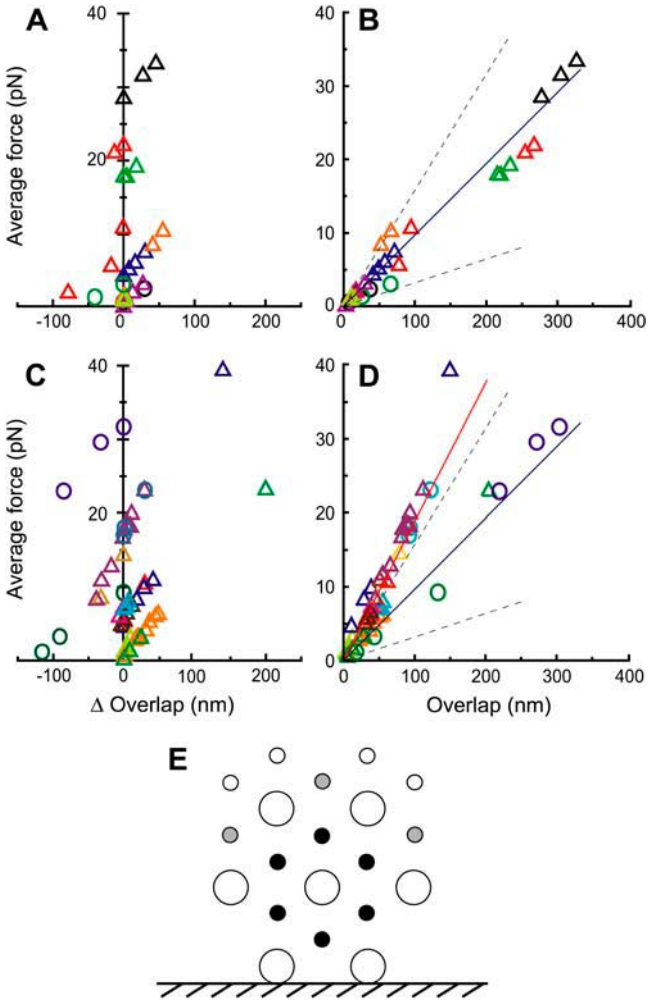

FIGURE 5 Length-force relationship in the A-band motility assay system. (*A* and *B*) Actin filaments interacted with the outer surface of the A-band (data were obtained from 10 different preparations). (*C* and *D*) Actin filaments interacted with the end plane of the A-band (data were obtained from 13 different preparations). (*A* and *C*) The change in overlap versus the average force. Each set of data points distinguished by color was obtained in one preparation by changing the stiffness of the optical tweezers (*triangles*) or by moving the sample stage (*circles*). The average force initially developed before the change in the stiffness or the movement of the stage is plotted on the ordinate. (*B* and *D*) Overlap versus the average force. Each data set in *A* and *C* was shifted in parallel to the abscissa, such that the approximate line determined for each data set by the least-squares method passed through the origin. (*B*) Length-force relationship obtained when an actin filament interacted with the outer surface of the A-band. The blue solid line, 0.097 pN/nm, indicates the mean of slopes. Two dashed lines, 0.097 ± (0.032 × 1.96) pN/nm, indicate the border of the 95% confidence interval of the population mean. (*D*) Length-force relationship obtained when an actin filament interacted with the end-plane of the A-band. A blue solid line and two dashed lines are identical to those in *B*. A red line indicates the mean of slopes for the data from outside the region surrounded by the two dashed lines. (*E*) Schematic illustration showing the geometry of the thick filaments (*open large circles*) and the actin filaments inside (*black circles*) and outside (*gray* and *open small circles*) the A-band.

TABLE 1 Summary of the mean force per unit length of overlap outside and inside the thick-filament lattice calculated from the slope for each set of data points in Fig. 5.

	Outside	Inside
	pN/nm	pN/nm
Outer surface of the A-band	0.097 ± 0.032 (10)	—
End-plane of the A-band	0.11 ± 0.028 (5)	0.19 ± .031 (8)

The values are given as mean ± SE with numbers of preparations, *n*, indicated in parentheses. Slopes were determined by the least-squares method. The data were obtained by the interaction of an actin filament with the outer surface or the end-plane of the A-band, which was determined by microscopic observation during the experiments according to the geometry of the actin filament and the A-band. The data obtained for the end-plane of the A-band were classified into two types, i.e., outside or inside the thick-filament lattice, according to the slope for the relationship of the average force versus overlap shown in Fig. 5 *D* (for more details, see the text).

significantly different from the data classified into the group having the smaller slope in Fig. 5, *B* and *D* ($P < 0.003$, verified by Mann-Whitney U-test). We therefore determined the force per unit length of the overlap from the values of the slopes as 0.19 ± 0.031 pN/nm (mean ± SE, $n = 8$). This is attributable to the force that is developed when the actin filament interacts at the center of the thick-filament triangular lattice (i.e., at the most stable position; see Fig. 5 *E*). The reason the force per unit length of overlap was smaller, ~1/2, outside than inside the A-band is probably that the number of thick filaments interacting with a single actin filament outside the A-band is 1/3–2/3 that inside (for the geometry of the thick-filament lattice, compare the *gray* and *open small circles* with the *filled circles* in Fig. 5 *E*).

The time average of the force generated by single myosin heads inside the A-band is estimated assuming that the actin filament is located at the most stable position in the thick-filament lattice. A thick filament (1.6 μm long) consists of 300 myosin molecules, implying that there are 150 myosin molecules (300 heads) in half a sarcomere. As a single actin filament is surrounded by three thick filaments (Fig. 5 *E*), we assumed that one-sixth (60°/360°) of the three thick filaments have a chance to interact with each actin filament. Consequently, we estimate that $300 \times 3/6 = 150$ myosin heads are available to each actin filament per half sarcomere. The effective length of the thick filament where myosin molecules are present in half a sarcomere is ~0.7 μm because myosin molecules are absent at the 0.2-μm-long central bare zone. Therefore, the average force per myosin head is estimated to be 0.19 pN/nm × 700 nm/150 = 0.9 pN. Note that 0.9 pN per myosin head corresponds to $\sim 2 \times 10^5$ N/m^2, the force developed in muscle, if the calculation is done as described above. In the muscle model systems, the isometric tension has been estimated as $1.05–2.20 \times 10^5$ N/m^2 at an ionic strength of 200 mM (7), and the average force per myosin head as 1.6 pN at 90 mM KCl (38).

The usual in vitro motility assay using randomly oriented myosin molecules showed the average force per myosin head

of 0.42 pN at 25 mM KCl (39) and 0.2 pN at 35 mM KCl (14). On the other hand, the in vitro assay using a synthetic myosin rod cofilament with oriented myosin molecules gave a value of 2.1 pN at 25 mM KCl (38). However, these values can not be directly compared with those obtained in muscle, as the developed force largely depends on ionic strength. Also, there is a possibility that the fraction of attached myosins differs between the different assays and conditions. As an actin filament is surrounded by the thick filaments in the A-band motility assay system, sustained force generation and sliding movements were possible even under a higher ionic strength, 100 mM KCl (ionic strength ~140 mM). Our result demonstrates that the force equivalent to that in muscle can be developed on a reconstituted pure actin filament in the thick-filament lattice structure.

Linear relationship between force and overlap

Fig. 5, *B* and *D* , indicate that the relationship between the average force and the overlap of an actin filament with the A-band is consistent with the linear length-tension relationship observed in an intact muscle fiber under an isometric condition (40). We stress here that this linear relationship was obtained only for the time-averaged force-versus-overlap relationship. In practice, the tension largely fluctuated around the average force, indicating that the force instantaneously developed is much higher than the average. Such a nonlinear feature of tension (and length) fluctuation should be examined in future by data analysis with higher time resolution.

The linear relationship was retained irrespective of whether the interaction occurred outside (Fig. 5 *B*) or inside (Fig. 5 *D*) the A-band. These results imply that, at least on average, the total force can be described as the simple sum of the forces generated by each myosin molecule. However, because the trap force was not sufficiently large, this relationship could only be obtained at the end region of the A-band, i.e., less than half of a full overlap. We have not yet examined whether the linear relationship obtained here is extrapolated up to 700 nm (the edge of the pseudo-H-zone). Also, we need to examine whether no cooperativity exists among cross-bridges even after the regulatory proteins are reconstituted, or under the conditions intermediate between contraction and relaxation at which, for example, spontaneous oscillatory contraction occurs (23).

Force fluctuations

In the 1970s, Borejdo and Morales (25) tried to determine the rate constants for the elementary processes of each myosin molecule interacting with the thin filament by analyzing force fluctuation under the steady state in a muscle fiber. However, the amplitude of fluctuation was too small compared to the force level because of a large number of myosin molecules (>10 million) working in their system. Therefore, artifacts associated with the experimental procedure could not be absolutely excluded, as was mentioned by the authors. In contrast, here we observed large back-and-forth displacement of a single actin filament accompanied by a large change in developed force. This may be attributable to the number fluctuation of the force-generating cross-bridge because the number of available myosin heads is small, ~10. Our A-band motility assay system is suitable for such analysis, as the force fluctuations can be recorded with sufficient sensitivity on a single actin filament due to the small number of interacting myosin molecules. The next step for us is to improve time resolution, because the video rate was too slow to analyze the actual force fluctuations due to the elementary steps of each myosin molecule. We also need to achieve an isometric condition for this purpose, which when accomplished should make it possible to study the response against quick stretch and quick release, leading to a more detailed analysis of the mechanochemical coupling mechanism in muscle contraction in an ordered array of myosin molecules.

CONCLUSION

We have described a new motility assay system, the A-band motility assay. Its most important feature is that it makes possible study of the characteristics of the muscle contractile system at a single-actin filament level under physiological conditions. The force generation on a single reconstituted actin filament and its displacement can be measured in the minimum unit of striated muscle with an accuracy of within subpiconewtons and a few nanometers, respectively. The experiments can be performed at nearly physiological solvent conditions without the detachment of the actin filament from myosin molecules. Further, it will be possible to examine the roles of an actin filament with and without regulatory proteins in the mechanism of muscle contraction and regulation by using genetically engineered or chemically modified actin filaments and regulatory proteins. In this respect, our A-band motility assay system is complementary to the contractile system of muscle in which thin filaments are reconstituted (34,35).

SUPPLEMENTARY MATERIAL

An online supplement to this article can be found by visiting BJ Online at http://www.biophysj.org.

We thank Mr. T. Iga of Waseda University for his efforts at the initial stage of this research project.

This research was partly supported by Grants-in-Aid for Specially Promoted Research, from the 21st Century COE Program (Physics of Self-Organization Systems) at Waseda University, and from the Bio-venture Project from the Ministry of Education, Sports, Culture, Science and Technology of Japan to S.I., and by Grants-in-Aid for Special Research Projects from Waseda University (2002A-867 and 2004A-226), from the 21st Century COE program (Physics of Self-Organization Systems) at Waseda University, and from the New Technology Development Project of the Ministry of Education, Sports, Culture, Science and Technology of Japan to M.S.

REFERENCES

1. Natori, R. 1954. The role of myofibrils, sarcoplasm and sarcolemma. *Jikeikai Med. J.* 1:18–28.
2. Nakajima, Y., and M. Endo. 1973. Release of calcium induced by 'depolarisation' of the sarcoplasmic reticulum membrane. *Nat. New Biol.* 246:216–218.
3. Irving, M., G. Piazzesi, L. Lucii, Y.-B. Sun, J. J. Harford, I. M. Dobbie, M. A. Ferenczi, M. Reconditi, and V. Lombardi. 2000. Conformation of the myosin motor during force generation in skeletal muscle. *Nat. Struct. Biol.* 7:482–485.
4. Corrie, J. E. T., B. D. Brandmeier, R. E. Ferguson, D. R. Trentham, J. Kendrick-Jones, S. C. Hopkins, U. A. Van der Heide, Y. E. Goldman, C. Sabido-David, R. E. Dale, S. Criddle, and M. Irving. 1999. Dynamic measurement of myosin light-chain-domain tilt and twist in muscle contraction. *Nature.* 400:425–430.
5. Piazzesi, G., M. Reconditi, M. Linari, L. Lucil, Y.-B. Sun, T. Narayanan, P. Boesecke, V. Lombardi, and M. Irving. 2002. Mechanism of force generation by myosin heads in skeletal muscle. *Nature.* 415:659–662.
6. Anazawa, T., K. Yasuda, and S. Ishiwata. 1992. Spontaneous oscillation of tension and sarcomere length in skeletal myofibrils. *Biophys. J.* 61:1099–1108.
7. Friedman, A. L., and Y. E. Goldman. 1996. Mechanical characterization of skeletal muscle myofibrils. *Biophys. J.* 71:2774–2785.
8. Yanagida, T., M. Nakase, K. Nishiyama, and F. Oosawa. 1984. Direct observation of motion of single F-actin filaments in the presence of myosin. *Nature.* 307:58–60.
9. Kron, S. J., and J. A. Spudich. 1986. Fluorescent actin filaments move on myosin fixed to a glass surface. *Proc. Natl. Acad. Sci. USA.* 83: 6272–6276.
10. Funatsu, T., Y. Harada, M. Tokunaga, K. Saito, and T. Yanagida. 1995. Imaging of single fluorescent molecules and individual ATP turnovers by single myosin molecules in aqueous solution. *Nature.* 374:555–559.
11. Sase, I., H. Miyata, J. E. T. Corrie, J. S. Craik, and K. Kinosita, Jr. 1995. Real time imaging of single fluorophores on moving actin with an epifluorescence microscope. *Biophys. J.* 69:323–328.
12. Ashkin, A., J. M. Dziedzic, J. E. Bjorkholm, and S. Chu. 1986. Observation of a single-beam gradient force optical trap for dielectric particles. *Opt. Lett.* 11:288–290.
13. Ashkin, A., K. Schutze, J. M. Dziedzic, U. Euteneuer, and M. Schliwa. 1990. Force generation of organelle transport measured in vivo by an infrared laser trap. *Nature.* 348:346–348.
14. Kishino, A., and T. Yanagida. 1988. Force measurements by micromanipulation of a single actin filament by glass needles. *Nature.* 334: 74–76.
15. Ishijima, A., H. Kojima, T. Funatsu, M. Tokunaga, H. Higuchi, H. Tanaka, and T. Yanagida. 1998. Simultaneous observation of individual ATPase and mechanical events by a single myosin molecule during interaction with actin. *Cell.* 92:161–171.
16. Kitamura, K., M. Tokunaga, A. H. Iwane, and T. Yanagida. 1999. A single myosin head moves along an actin filament with regular steps of 5.3 nanometres. *Nature.* 397:129–134.
17. Nishizaka, T., R. Seo, H. Tadakuma, K. Kinosita, Jr., and S. Ishiwata. 2000. Characterization of single actomyosin rigor bonds: load dependence of lifetime and mechanical properties. *Biophys. J.* 79: 962–974.
18. Veigel, C., M. L. Bartoo, D. C. S. White, J. C. Sparrow, and J. E. Molloy. 1998. The stiffness of rabbit skeletal actomyosin cross-bridges determined with an optical tweezers transducer. *Biophys. J.* 75:1424–1438.
19. Molloy, J. E., J. E. Burns, J. Kendrick-Jones, R. T. Tregear, and D. C. S. White. 1995. Movement and force produced by a single myosin head. *Nature.* 378:209–212.
20. Mehta, A. D., J. T. Finer, and J. A. Spudich. 1997. Detection of single-molecule interactions using correlated thermal diffusion. *Proc. Natl. Acad. Sci. USA.* 94:7927–7931.
21. Finer, J. T., R. M. Simmons, and J. A. Spudich. 1994. Single myosin molecule mechanics: piconewton forces and nanometre steps. *Nature.* 368:113–119.
22. Miyata, H., H. Hakozaki, H. Yoshikawa, N. Suzuki, K. Kinosita, Jr., T. Nishizaka, and S. Ishiwata. 1994. Stepwise motion of an actin filament over a small number of heavy meromyosin molecules is revealed in an *in vitro* motility assay. *J. Biochem.* (*Tokyo*). 115:644–647.
23. Ishiwata, S., and K. Yasuda. 1993. Mechano-chemical coupling in spontaneous oscillatory contraction of muscle. *Phase Transit.* 45:105–136.
24. Tanaka, H., A. Ishijima, M. Honda, K. Saito, and T. Yanagida. 1998. Orientation dependence of displacements by a single one-headed myosin relative to the actin filament. *Biophys. J.* 75:1886–1894.
25. Borejdo, J., and M. F. Morales. 1977. Fluctuations in tension during contraction of single muscle fibers. *Biophys. J.* 20:315–334.
26. Suzuki, M., H. Fujita, and S. Ishiwata. 2003. Bio-nanomuscle project: contractile properties of single actin filaments in an A-band motility assay system. *In* Molecular and Cellular Aspects of Muscle Contraction. H. Sugi, editor. Kluwer Academic/Plenum Publishers, New York. 103–110.
27. Ishiwata, S., and T. Funatsu. 1985. Does actin bind to the ends of thin filaments in skeletal muscle? *J. Cell Biol.* 100:282–291.
28. Kondo, H., and S. Ishiwata. 1976. Uni-directional growth of F-actin. *J. Biochem.* (*Tokyo*). 79:159–171.
29. Suzuki, N., H. Miyata, S. Ishiwata, and K. Kinosita, Jr. 1996. Preparation of bead-tailed actin filaments: estimation of the torque produced by the sliding force in an in vitro motility assay. *Biophys. J.* 70:401–408.
30. Kurokawa, H., W. Fujii, K. Ohmi, T. Sakurai, and Y. Nonomura. 1990. Simple and rapid purification of brevin. *Biochem. Biophys. Res. Commun.* 168:451–457.
31. Horiuti, K. 1986. Some properties of the contractile system and sarcoplasmic reticulum of skinned slow fibres from Xenopus muscle. *J. Physiol.* (*Lond.*). 373:1–23.
32. Nishizaka, T., H. Miyata, H. Yoshikawa, S. Ishiwata, and K. Kinosita, Jr. 1995. Unbinding force of a single motor molecule of muscle measured using optical tweezers. *Nature.* 377:251–254.
33. Funatsu, T., H. Higuchi, and S. Ishiwata. 1990. Elastic filaments in skeletal muscle revealed by selective removal of thin filaments with plasma gelsolin. *J. Cell Biol.* 110:53–62.
34. Funatsu, T., T. Anazawa, and S. Ishiwata. 1994. Structural and functional reconstitution of thin filaments in skeletal muscle. *J. Muscle Res. Cell Motil.* 15:158–171.
35. Fujita, H., K. Yasuda, S. Niitsu, T. Funatsu, and S. Ishiwata. 1996. Structural and functional reconstitution of thin filaments in the contractile apparatus of cardiac muscle. *Biophys. J.* 71:2307–2318.
36. Ishiwata, S. 1981. Melting from both ends of an A-band in a myofibril. Observation with a phase-contrast microscope. *J. Biochem.* (*Tokyo*). 89:1647–1650.
37. Ishiwata, S., K. Muramatsu, and H. Higuchi. 1985. Disassembly from both ends of thick filaments in rabbit skeletal muscle fibers. An optical diffraction study. *Biophys. J.* 47:257–266.
38. Ishijima, A., H. Kojima, H. Higuchi, Y. Harada, T. Funatsu, and T. Yanagida. 1996. Multiple- and single-molecule analysis of the actomyosin motor by nanometer-piconewton manipulation with a microneedle: unitary steps and forces. *Biophys. J.* 70:383–400.
39. Ishijima, A., T. Doi, K. Sakurada, and T. Yanagida. 1991. Subpiconewton force fluctuations of actomyosin *in vitro*. *Nature.* 352:301–306.
40. Gordon, A. M., A. F. Huxley, and F. J. Julian. 1966. The variation in isometric tension with sarcomere length in vertebrate muscle fibres. *J. Physiol.* (*Lond.*). 184:170–192.